Cell Reports
Article

Silencing the Majority of Cerebellar Granule Cells Uncovers Their Essential Role in Motor Learning and Consolidation

Elisa Galliano,[1,6] Zhenyu Gao,[1,6] Martijn Schonewille,[1,6] Boyan Todorov,[2] Esther Simons,[1] Andreea S. Pop,[1] Egidio D'Angelo,[4] Arn M.J.M. van den Maagdenberg,[2,3] Freek E. Hoebeek,[1,*] and Chris I. De Zeeuw[1,5,*]
[1]Department of Neuroscience, Erasmus MC Rotterdam, 3015GE Rotterdam, the Netherlands
[2]Department of Human Genetics
[3]Department of Neurology
Leiden University Medical Center, 2333ZA Leiden, the Netherlands
[4]Department of Neuroscience and Brain Connectivity Center (BCC), University of Pavia and IRCCS C. Mondino, 27100 Pavia, Italy
[5]Netherlands Institute for Neuroscience, Royal Netherlands Academy of Arts & Sciences, 1105BA Amsterdam, the Netherlands
[6]These authors contributed equally to this work
*Correspondence: f.hoebeek@erasmusmc.nl (F.E.H.), c.dezeeuw@erasmusmc.nl (C.I.D.Z.)
http://dx.doi.org/10.1016/j.celrep.2013.03.023

SUMMARY

Cerebellar granule cells (GCs) account for more than half of all neurons in the CNS of vertebrates. Theoretical work has suggested that the abundance of GCs is advantageous for sparse coding during memory formation. Here, we minimized the output of the majority of GCs by selectively eliminating their $Ca_V2.1$ (P/Q-type) Ca^{2+} channels, which mediate the bulk of their neurotransmitter release. This resulted in reduced GC output to Purkinje cells (PCs) and stellate cells (SCs) as well as in impaired long-term plasticity at GC-PC synapses. As a consequence modulation amplitude and regularity of simple spike (SS) output were affected. Surprisingly, the overall motor performance was intact, whereas demanding motor learning and memory consolidation tasks were compromised. Our findings indicate that a minority of functionally intact GCs is sufficient for the maintenance of basic motor performance, whereas acquisition and stabilization of sophisticated memories require higher numbers of normal GCs controlling PC firing.

INTRODUCTION

Over half of all neurons of the CNS are cerebellar GCs (Williams and Herrup, 1988). These densely packed, small cells constitute the main input stage of the cerebellar cortex, and they are characterized by a peculiar morphology, which has been preserved throughout vertebrate phylogeny (Eccles, 1969). Each of the four short dendrites of a GC receives input from a single afferent mossy fiber, and their cell body gives rise to an ascending axon that bifurcates into two parallel fibers (PFs). GCs' unique design is probably essential to confer them high sensitivity for individual afferents (Chadderton et al., 2004; Ekerot and Jörntell, 2008; Rothman et al., 2009). However, the functional consequence of their striking abundance remains elusive. Theoreticians have hypothesized that it would allow the cerebellum to exploit the advantages of sparse coding in terms of memory storage capacity (Schweighofer et al., 2001). Yet, it remains to be proven whether this extreme GC abundance is indeed essential to encode the wide range of information presented to the cerebellar cortex into an adaptable output that controls motor behavior.

Previous investigations have studied cerebellum-dependent behavior in mouse models in which the output of the granular layer was completely abolished, either by eliminating all GCs (De Zeeuw et al., 2004; Sidman et al., 1965) or by blocking neurotransmitter release from all GCs (Kim et al., 2009; Wada et al., 2007). These robust interventions induced severe behavioral symptoms including ataxia and hypotonia (De Zeeuw et al., 2004; Kim et al., 2009). Yet, by completely interrupting the flow of information from the cerebellar input stage to the output stage, these studies cannot address the question of why vertebrates have this enormous amount of GCs. Thus, to better understand the evolutionary preservation of the abundance of cerebellar GCs, a preferable strategy would be to tackle the output of most, but not all, GCs. Moreover, since a structural elimination of granule cells, such as in the *weaver* mouse mutant, can cause structural, secondary pathological processes in their target neurons (Maricich et al., 1997), it is probably advantageous to create a mouse mutant in which the output of the majority of GCs is affected functionally rather than structurally.

To achieve this goal, we took advantage of incomplete expression of Cre recombinase using the *Cre*-LoxP system (Tymms and Kola, 2001) and generated a subtotal conditional granule-cell-specific knockout line of P/Q-type voltage-gated calcium channels (VGCCs), which normally mediate ~90% of neurotransmitter release from GC axons during adulthood (D'Angelo et al., 1997; Mintz et al., 1995). By cross-breeding the floxed mouse line targeted for exon 4 of *Cacna1a*, i.e., the gene encoding the pore-forming α1 subunit of P/Q-type VGCCs (Todorov et al., 2006), with mutant mice that specifically express Cre

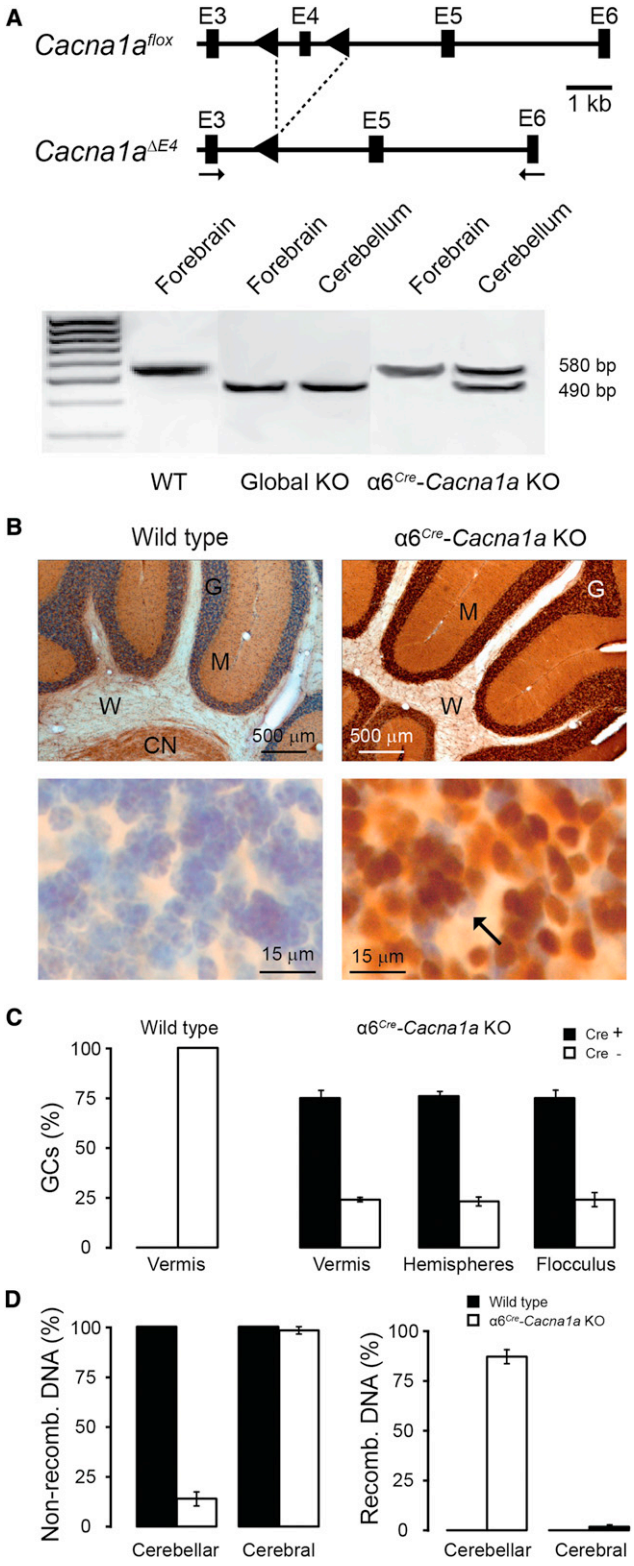

Figure 1. *Cre*-LoxP Strategy to Obtain Granule-Cell-Specific *Cacna1a* Knockout Mice

(A) Top: Representation of relevant part of *Cacna1a*^{flox} allele; black boxes indicate exons E3-E6, triangles indicate relative position of LoxP sites; arrows indicate position of exotic primers. Bottom: RT-PCR of wild-type cerebellar RNA amplified a 580 bp fragment. Global KO of *Cacna1a*^{flox} was induced by crossing with conditional EIIA-driven *Cre* mice (see Extended Experimental Procedures), which resulted in 490 bp fragments that lack exon 4 in both forebrain and cerebellum. In α6^{Cre}-*Cacna1a* KO mice, RT-PCR of forebrain RNA amplified a wild-type 580 bp fragments; both 580 and 490 bp fragments were found in the cerebellum, suggesting cell-specific deletion of exon 4.

(B) Immunohistochemical staining using anti-Cre antibodies show GC-specific expression of Cre. Top: Cre is specifically expressed in the granule cell layer in α6^{Cre}-*Cacna1a* KO. M, molecular layer; G, granule cell layer; W, white matter; CN, cerebellar nuclei. Bottom: Cre is expressed in most, but not all GCs. Arrow indicates a Cre-negative GC.

(C) Quantification of GCs negative for Cre immunohistochemistry in tissue from wild-type vermis and α6^{Cre}-*Cacna1a* KO cerebellar vermis, hemisphere, and flocculus. See also Figure S1 and Table S1.

(D) Quantitative RT-PCR products of cerebellar tissue show that in α6^{Cre}-*Cacna1a* KO mice the recombined DNA fraction dominates the non-recombined fraction, in contrast to cerebral cortex tissue and lung tissue (data not shown).

Values: mean ± SEM; p values are described in the main text.

recombinase in the majority of cerebellar GCs (α6^{Cre}) (Aller et al., 2003), we generated α6^{Cre}-*Cacna1a* KO. Our data demonstrate that subtotal α6^{Cre}-*Cacna1a* KO mice show no defects at the level of cytoarchitecture or motor performance, but have a compromised capability for adaptation and consolidation, thereby redefining the role of GCs in cerebellar function.

RESULTS

α6^{Cre}-Cacna1a KO Mice Lack *Cacna1a* Gene from Most, but Not All, GCs

Using the imperfect *Cre*-LoxP system (Tymms and Kola, 2001), we generated a line of α6^{Cre}-*Cacna1a* KO mice, in which most, but not all, GCs express Cre recombinase (Figure 1A). Therefore, a smaller portion of the α6^{Cre}-*Cacna1a* KO granule cell population still harbored the (floxed) *Cacna1a* gene and expressed P/Q-type VGCCs. To confirm presence of Cre-negative neurons in α6^{Cre}-*Cacna1a* KO mice, we performed immunohistochemical staining using an antibody against Cre recombinase. As expected, all GCs from wild-type (WT) mice and a minority of the GCs in the α6^{Cre}-*Cacna1a* KO mice were Cre negative (Figure 1B). Quantification across various cerebellar regions revealed that in α6^{Cre}-*Cacna1a* KO mice 75% of GCs were Cre positive (Figure 1C). To confirm the functionality of the expressed Cre recombinase, we performed a real-time quantitative PCR on tissue samples of α6^{Cre}-*Cacna1a* KO mice and control littermates using primers designed to detect alleles that incorporate two LoxP sites (i.e., nonrecombined DNA with the endogenous *Cacna1a* gene) or alleles that contain a single LoxP site (i.e., recombined DNA without exon 4 of the *Cacna1a* gene). We did not detect recombined DNA (i.e., <2%) in the cerebral cortex of either genotypes or in the cerebellum of WT, while in the cerebellar cortex of α6^{Cre}-*Cacna1a* KO mice the predominant fraction was recombined DNA (86.2% ± 3.5% recombined versus 13.8% ± 3.5% nonrecombined; Figure 1D). Thus, we successfully created a mouse line in which we had a mixture of GCs (ranging from an average of 75% to 86%) that lack the gene coding for the

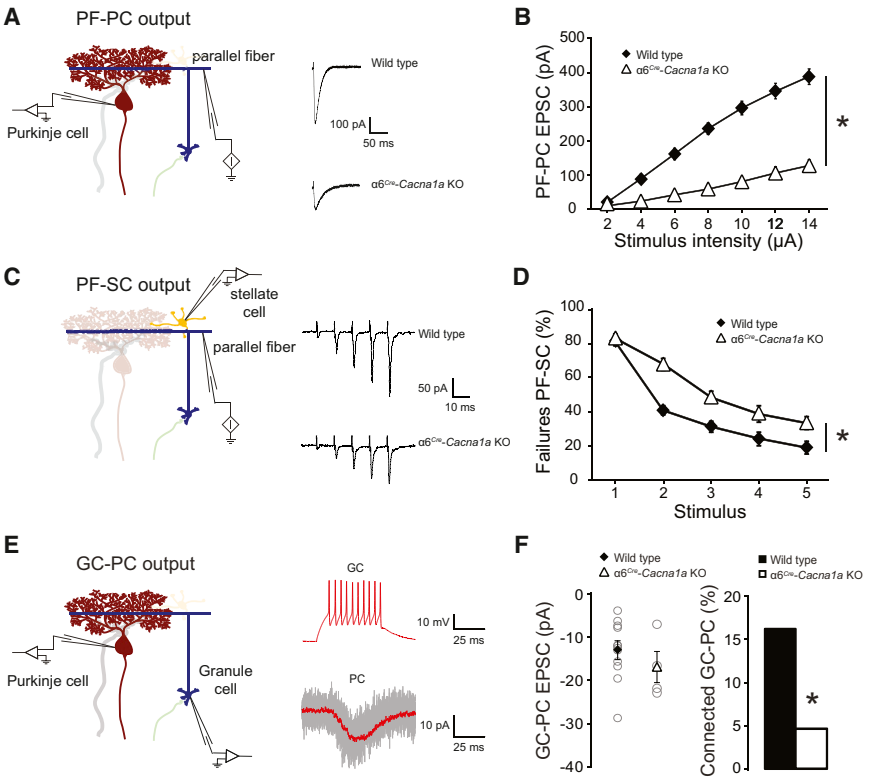

Figure 2. Cerebellar GCs' Output Is Minimized in $\alpha6^{Cre}$-*Cacna1a* KO Mice

(A, C, and E) Representation of connectivity within cerebellar cortex and positions of recording (triangle) and stimulus (diamond) pipettes. For a detailed description of GC, PC, and SC intrinsic properties and MF-GC synapse, see Figures S2, S3, and Tables S2 and S3.

(A) Parallel fiber-Purkinje cell (PF-PC) output. Insets: typical PC responses to a single-pulse PF beam stimulation of 10 μA for wild-type (top) and $\alpha6^{Cre}$-*Cacna1a* KO mice (bottom).

(B) Average amplitude of excitatory postsynaptic currents (EPSCs) to stimuli of increasing intensity for wild-type (black diamond, n = 13) and $\alpha6^{Cre}$-*Cacna1a* KO mice (white triangle, n = 9).

(C) Parallel fiber-stellate cell (PF-SC) output. Insets: averages of 30 repetitive PF-SC EPSC recordings in response to train stimuli (five pulses at 100 Hz) for wild-type (top) and $\alpha6^{Cre}$-*Cacna1a* KO mice (bottom).

(D) Percentage of failures recorded in SCs in response to PF stimulation is significantly increased in $\alpha6^{Cre}$-*Cacna1a* KO mice (white triangle, n = 12) compared to wild-type (black diamond, n = 9); number of failures to the first stimulus is set at 80% (see Extended Experimental Procedures). Miniature PF-SC EPSCs are shown in Figure S4 and quantified in Table S4.

(E) Granule cell-Purkinje cell output (GC-PC). Insets, top: traces of a connected GC-PC pair from wild-type. A train of action potentials of ~200 Hz elicited by somatic current injection in the GC (red trace) induced postsynaptic responses in the PC. Bottom: Red trace indicates the averaged response of ten repetitive sweeps (gray traces) of GC-PC EPSC.

(F) Left: summary of EPSC amplitudes in PCs evoked by activation of a single GC for wild-type (open circles and black diamond, n = 11 out of the total of 68 paired recordings) and $\alpha6^{Cre}$-*Cacna1a* KO (open circles and white triangle, n = 4 out of the total of 81 paired recordings) using paired GC-PC whole-cell recordings. Right: Percentage of connected GC-PC pairs with detectable EPSC responses.

Values: mean ± SEM; asterisks: significant differences; p values are described in the main text.

pore-forming subunit of P/Q-type VGCCs and GCs (ranging from an average of 25%–14%) that still express this gene.

Impaired Neurotransmission in Most GC Axons

In mature granule cells, the P/Q-type VGCC is expressed only at their axon terminals (D'Angelo et al., 1997), where it mediates the bulk of the neurotransmitter release (Mintz et al., 1995). Ablation of synaptic P/Q-type VGCC from the majority of GCs caused no gross anatomical alteration in the cerebellar circuitry of $\alpha6^{Cre}$-*Cacna1a* KO animals (Figure 1B) and the ultrastructure, electroresponsiveness, and input integration properties of their GCs were intact (all p values > 0.1; Figures S1 and S2; Tables S1 and S2). We next recorded excitatory postsynaptic currents (EPSCs) in both PCs and stellate cells (SCs) (Figures 2A–2D), which showed no sign of secondary compensatory mechanisms in their intrinsic activity (Figure S3; Table S3). Whole-cell recordings showed that following stimulation of PFs, EPSC amplitudes in PCs were significantly lower in $\alpha6^{Cre}$-*Cacna1a* KO mice at stimulus intensities >2 μA ($p < 0.001$; repeated-measures ANOVA). Likewise, average postsynaptic responses evoked by activation of PF-SC synapses were smaller and the failure rate at PF-SC synapses was significantly higher in $\alpha6^{Cre}$-*Cacna1a* KO mice ($p = 0.04$; repeated-measures ANOVA). To investigate whether this reduction in postsynaptic responses to GC activation was due to a decrease in the output of all GCs or due to a lack of output of a subset of GCs, we evoked a 200 ms train of action potentials at 200 Hz in individual GCs and recorded the responses in a surrounding PC using paired whole-cell recordings (Figure 2E). Eleven of the 68 paired GC-PC recordings in WTs showed an evoked synaptic response in PCs, whereas in $\alpha6^{Cre}$-*Cacna1a* KO mice only four of the 81 paired recordings revealed an evoked response (WT versus KO, p = 0.006; binomial test). Notably, the maximal evoked response in $\alpha6^{Cre}$-*Cacna1a* KO mice did not differ from that in WTs ($p = 0.33$; Figure 2F). These results are in line with the immunohistochemical and genetic analysis (Figure 1) and indicate that in $\alpha6^{Cre}$-*Cacna1a*KO animals the majority of GCs appears largely disconnected from their downstream target neurons.

Remaining Neurotransmitter Release Arises Mainly from Functionally Intact GCs

Our data described above not only show that in $\alpha6^{Cre}$-*Cacna1a* KO mice the output of the GC layer is greatly reduced, but also suggest that a subset of GCs remains at least partially, functionally intact. To verify these findings, we recorded the responses in PCs to PF beam stimulation with two pulses separated by an increasing time interval (Figure 3A). We found no significant differences among these paired-pulse ratios of $\alpha6^{Cre}$-*Cacna1a*

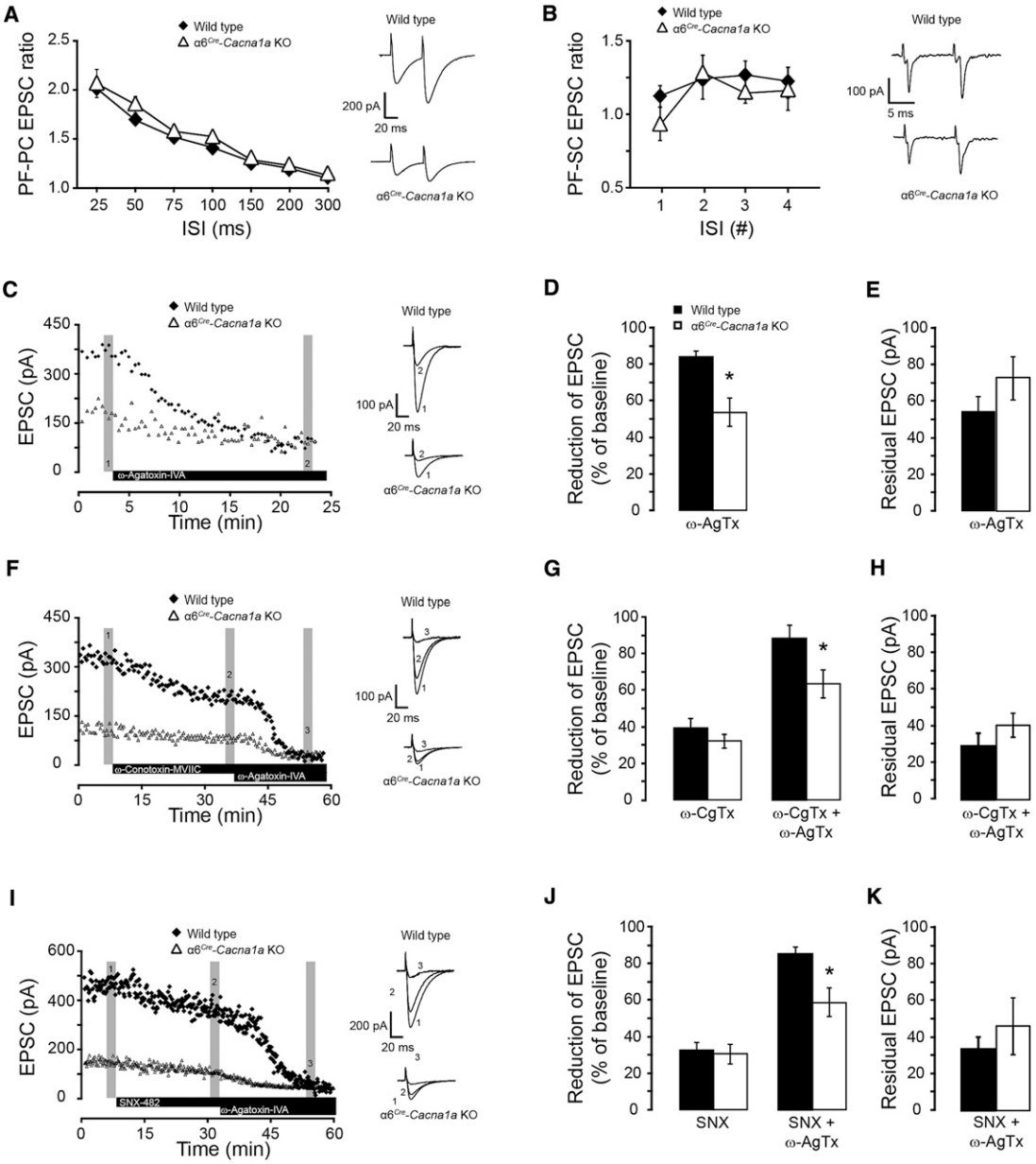

Figure 3. Remaining GC Output Is Functionally Intact and the Lack of P/Q-type Channels Appears Uncompensated

(A) Parallel fiber to Purkinje cell (PF-PC) EPSC ratio between second and first response to double stimuli with 25–300 ms interstimulus intervals in wild-type (black diamond, n = 10) and $\alpha6^{Cre}$-*Cacna1a* KO (white triangle, n = 17) mice. Insets: examples at 50 ms interstimulus interval.

(B) PF-SC EPSC ratio between consecutive responses during a 100 Hz stimulus train of five pulses for wild-type (n = 9) and $\alpha6^{Cre}$-*Cacna1a* KO mice (n = 12). Insets: typical examples.

(C) PF-PC EPSC amplitude in PCs before (1) and after (2) application of ω-Agatoxin IVA (P/Q-type Ca^{2+}-channel blocker). Insets: PF-PC EPSCs at indicated time points for wild-type (top) and $\alpha6^{Cre}$-*Cacna1a* KO mice (bottom). Note the differences between wild-type and $\alpha6^{Cre}$-*Cacna1a* KO mice in initial amplitude and absolute effects of toxins.

(D) The average PF-PC EPSC component sensitive to the direct application of ω-Agatoxin IVA in wild-type (black, n = 7) and $\alpha6^{Cre}$-*Cacna1a* KO mice (white, n = 9).

(E) Residual EPSC (in pA) for wild-type and $\alpha6^{Cre}$-*Cacna1a* KO mice after application of ω-Agatoxin IVA.

(F) PF-PC EPSC amplitude in PCs before (1) and after application of ω-Conotoxin GVIA (N-type-specific Ca^{2+}-channel blocker) (2) and ω-Agatoxin IVA (3).

(G) The average PF-PC EPSC component sensitive to application of ω-Conotoxin GVIA (left) and additional application of ω-Agatoxin IVA (right) in wild-type (black, n = 8) and $\alpha6^{Cre}$-*Cacna1a* KO (white, n = 6) mice.

(H) Residual EPSC for wild-type and $\alpha6^{Cre}$-*Cacna1a* KO mice after co-application of ω-Conotoxin GVIA and ω-Agatoxin IVA.

(I) Similar to (F) for subsequent application of SNX-482 (R-type Ca^{2+}-channel blocker) and ω-Agatoxin IVA.

(J and K) Similar to (G) and (H) for subsequent application of SNX-482 and ω-Agatoxin IVA for wild-type (black, n = 8) and $\alpha6^{Cre}$-*Cacna1a* KO mice (white, n = 8).

Values: mean ± SEM; asterisks: significant differences; p values are described in the main text.

KOs and WT (p = 0.3; repeated-measures ANOVA; Figure 3A). This form of short-term plasticity also appeared normal at GC-SC synapses when tested for interstimulus intervals of 10 and 20 ms (all p values >0.15, repeated measures ANOVA; Figure 3B shows 10 ms interval). These data suggest that those GC terminals that revealed neurotransmission show normal levels of Ca^{2+} homeostasis.

Next, we evaluated the contribution of each type of VGCC to GC transmitter release (i.e., P/Q-, N-, and R-type; Mintz et al., 1995; Myoga and Regehr, 2011) by applying channel-specific blockers while recording from PCs and stimulating PFs (Figures 3C–3K). Application of ω-Agatoxin-IVA, which blocks P/Q-type channels, reduced PF-evoked EPSCs in WT significantly more than in $\alpha6^{Cre}$-*Cacna1a* KO (p = 0.004), whereas the remaining EPSC amplitude was not significantly different between $\alpha6^{Cre}$-*Cacna1a* KO and WT (p = 0.23). In contrast, application of ω-Conotoxin-MVIIC (N-type blocker) or SNX-482 (R-type blocker) revealed no significant differences between $\alpha6^{Cre}$-*Cacna1a* KO and WT (p = 0.35 and p = 0.78, respectively), which suggests that the lack of P/Q-type channels in $\alpha6^{Cre}$-*Cacna1a* KO did not trigger a pronounced compensatory increase in N- or R-type-mediated neurotransmitter release. While coapplication of ω-Conotoxin or SNX-482 with ω-Agatoxin returned a significant result in the relative residual component (p = 0.014 and p = 0.031, respectively), the absolute residual component measured in pA did not differ between $\alpha6^{Cre}$-*Cacna1a* KO and WT (p = 0.40 and p = 0.45, respectively). Thus, although the source of these residual amplitudes remains to be identified in both $\alpha6^{Cre}$-*Cacna1a* KO and WT, our data obtained with blockers are in line with those on paired-pulse ratios at GC-PC and GC-SC synapses, which together indicate that the remaining neurotransmitter release from GCs in $\alpha6^{Cre}$-*Cacna1a* KO's appears largely intact.

Although $\alpha6^{Cre}$-*Cacna1a* KO mutants do not show an altered contribution of non-P/Q-type channels to evoked neurotransmitter release, hypothetically, the lack of functional P/Q-type channels could alter the release machinery downstream of Ca^{2+} influx. To evaluate such a potentially compensatory effect we recorded miniature (m)EPSCs in SCs, which mostly occur as a result of stochastic fusion of vesicles with the synaptic membrane, i.e., a Ca^{2+}-independent process (Chen and Regehr, 1997). In the presence of tetrodotoxin (TTX), which blocks action potential mediated transmitter release, we found neither the frequency, nor the amplitude or kinetics of such mEPSCs to be significantly different in $\alpha6^{Cre}$-*Cacna1a* KO mice (all p values >0.16; Figure S4; Table S4). Moreover, in the absence of TTX we occasionally recorded high-frequency EPSCs in both WT and $\alpha6^{Cre}$-*Cacna1a* KO SCs (Figure S4), which are characteristic of normal GC activity (Chadderton et al., 2004) and thus provide further support for the notion that the remaining transmitter release from GCs in $\alpha6^{Cre}$-*Cacna1a* KO mice appears functionally intact.

No Changes in Motor Performance

To assess the impact of a substantially reduced GC output on cerebellar-dependent behavior, we first studied baseline motor performance of $\alpha6^{Cre}$-*Cacna1a* KO mice using a battery of quantitative tests. Remarkably, the performance of $\alpha6^{Cre}$-*Cacna1a* KO mice was indistinguishable from that of WT littermates in the open field (p = 0.21 for both distance traveled and average speed), rotarod (4–40 rpm in 300 s: p = 0.83; 2–80 rpm in 300 s: p = 0.23), balance beam (p = 0.27, repeated-measures ANOVA), and Erasmus Ladder task (p = 0.97, repeated-measures ANOVA) (Figures 4A–4D). In addition, we evaluated oculomotor activity, which is particularly sensitive to cerebellar deficits (Schonewille et al., 2010). Both gain and phase values during the optokinetic reflex (OKR) (p = 0.25 and p = 0.43, respectively; repeated-measures ANOVA), vestibulo-ocular reflex (VOR) in the dark (p = 0.49 and p = 0.35), and VOR in the light (visually enhanced VOR [VVOR]; p = 0.52 and p = 0.74), all recorded at 0.1–1.0 Hz with 5° amplitude, did not differ significantly between $\alpha6^{Cre}$-*Cacna1a* KO and WT mice (Figures 4E–4G). To further challenge the animals, we increased the difficulty of the OKR experiments, during which the mice were subjected to higher stimulus frequencies (up to 1.6 Hz) and higher stimulus amplitudes (up to 25°) while maintaining peak drum velocity (Figure 4H). Here, too, we observed no significant differences in gain (p = 0.21) or phase (p = 0.54).

Deficits in Motor Learning and Consolidation

To find out to what extent the GC output is relevant for motor learning and storage of procedural memories (De Zeeuw et al., 2011), we studied the ability of $\alpha6^{Cre}$-*Cacna1a* KO mice to learn to walk on a fast-accelerating rotarod and to adapt their VOR. With regard to locomotion learning (Figures 5A–5C), $\alpha6^{Cre}$-*Cacna1a* KO learned significantly less (p = 0.02; ANOVA for repeated measures) than their wild-type littermates on a fast-accelerating rotarod (4–80 rpm in 300 s) over eight consecutive training days. In addition, we quantified the maximum speed that was reached at the end of the training sessions and found that $\alpha6^{Cre}$-*Cacna1a* KO mice reached a significantly lower level (p = 0.02) than controls. With regard to VOR learning, the amplitude of the VOR in $\alpha6^{Cre}$-*Cacna1a* KO mice decreased to similar levels as that in WT mice (p = 0.9; repeated-measures ANOVA) during the first session of gain-decrease training (Figures 5D and 5E). However, when the animals were tested again after spending 23 hr in the dark, the VOR gain of $\alpha6^{Cre}$-*Cacna1a* KO mice had returned to near-baseline levels (p = 0.22; baseline versus next day, paired Student's t test), whereas that of WT mice was consolidated for ~60% (p = 0.02; $\alpha6^{Cre}$-*Cacna1a* KO versus WT) (Figures 5E and 5F). During VOR gain-increase and phase-increase training (Figures 5G–5L), which can be expected to be more sensitive to disruptions in cerebellar circuitry function (Hansel et al., 2006; Schonewille et al., 2010), $\alpha6^{Cre}$-*Cacna1a* KO mice showed immediate significant impairments in acquisition and consolidation compared to WT mice (p = 0.005 and p = 0.045 for gain-increase and phase-increase training, respectively; p = 0.046 for consolidation following phase-increase training, repeated-measures ANOVA; gain-increase consolidation values could not be determined for $\alpha6^{Cre}$-*Cacna1a* KO due to lack of learning). Moreover, when we subjected animals to an extended training with a phase-reversal paradigm repeated for four consecutive days, $\alpha6^{Cre}$-*Cacna1a* KO mice not only showed significantly impaired learning (p = 0.015 for days 3–5), but also a persistent problem with consolidation (p = 0.036 for days 2–5) (Figures 5M–5O and S5). Finally, given that OKR adaptation often occurs as a corollary effect of vestibular training (van Alphen and De Zeeuw, 2002), we measured OKR gain at the end

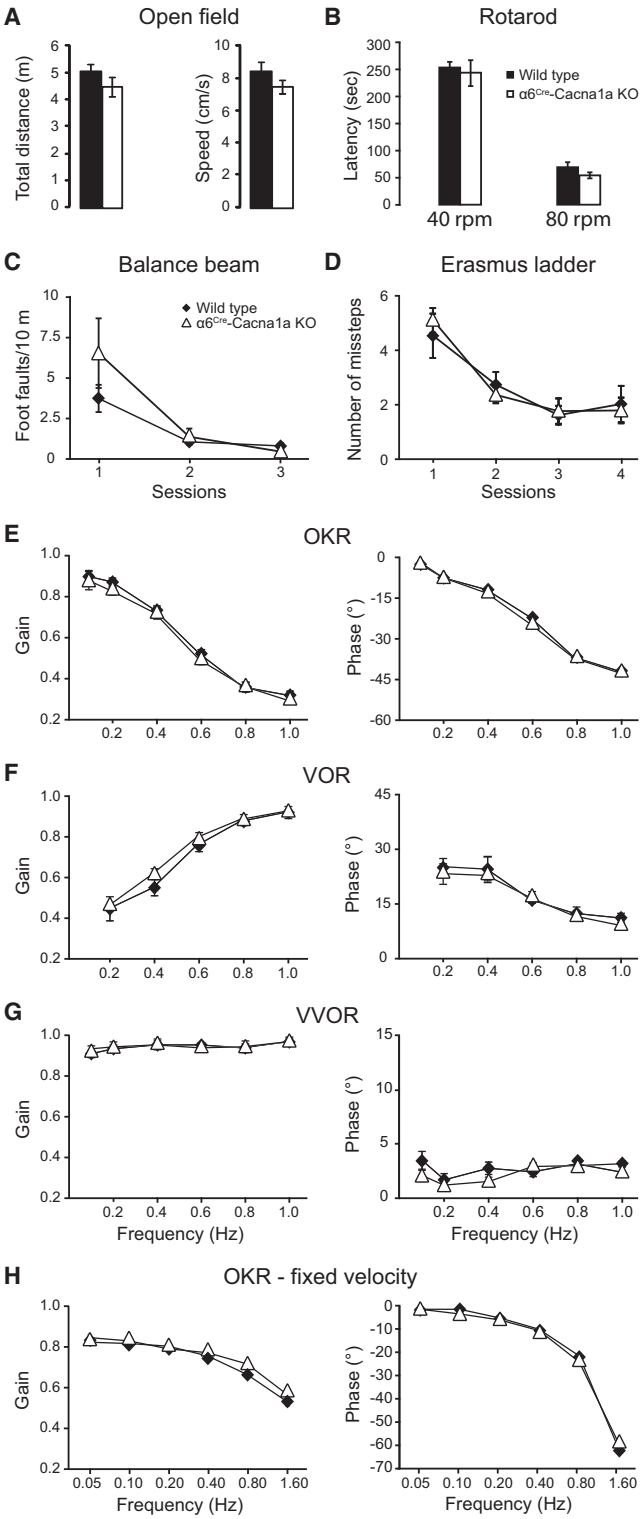

Figure 4. $\alpha6^{Cre}$-*Cacna1a* KO Mice Show Normal Motor Performance

(A) Distance traveled and average speed in open field for wild-type (black, n = 10) and $\alpha6^{Cre}$-*Cacna1a* KO mice (n = 11).

(B) Latency to fall from a rotating rod that accelerates in 300 s to either 40 rpm (left) or 80 rpm (right) for wild-type (n = 5 and n = 7, respectively) and $\alpha6^{Cre}$-*Cacna1a* KO mice (n = 5 and n = 6, respectively).

(C) Quantification of number of missteps on a narrow beam for wild-type (diamond, n = 9) and $\alpha6^{Cre}$-*Cacna1a* KO mice (triangle, n = 9).

(D) Quantification of number of missteps on Erasmus ladder for wild-type (diamond, n = 8) and $\alpha6^{Cre}$-*Cacna1a* KO mice (triangle, n = 8).

(E–G) Baseline compensatory eye movements quantified by gain (left) and phase (right) for wild-type (n = 13) and $\alpha6^{Cre}$-*Cacna1a* KO mice (n = 10): (E) optokinetic reflex (OKR); (F) vestibulo-ocular reflex (VOR); (G) visually enhanced VOR (VVOR).

(H) Fixed-velocity (8°/s) OKR.

Values: mean ± SEM; p values are described in the main text.

of our VOR training. In $\alpha6^{Cre}$-*Cacna1a* KO mice, both the VOR gain-increase and VOR phase-reversal protocol resulted in increased OKR gain values (VOR gain increase, $p < 0.001$; VOR phase reversal, $p = 0.06$; repeated-measures ANOVA), but these increases were significantly less than those in WT mice (all p value < 0.015; repeated-measures ANOVA) (Figure S5).

PF-PC Synaptic Plasticity Is Impaired While PC Intrinsic Plasticity Is Intact

The observation that some forms of motor learning are impaired in $\alpha6^{Cre}$-*Cacna1a* KO mice raises the possibility that plasticity is impaired at the PF-PC synapse, which is regarded as one of the key synapses for cerebellar learning (Gao et al., 2012; Ito, 2002). The induction of postsynaptic long-term potentiation (LTP) and that of postsynaptic long-term depression (LTD) at the PF-PC synapse of $\alpha6^{Cre}$-*Cacna1a* KO mice were both significantly impaired (for LTP in $\alpha6^{Cre}$-*Cacna1a* KO mice versus that in WT, $p = 0.01$; for LTD, $p = 0.02$; Figures 6A and 6B). Instead, following induction of intrinsic plasticity (Belmeguenai et al., 2010) PCs in $\alpha6^{Cre}$-*Cacna1a* KO and WT showed similar changes in response to injected currents ($p = 0.6$) (Figure 6C). Our results show that postsynaptic plasticity at PF-PC inputs is minimal in $\alpha6^{Cre}$-*Cacna1a* KO, but that PCs are still able to respond to those inputs with a plastic change of their electroresponsiveness.

Both Modulation and Regularity of Purkinje Cell Activity Are Affected

To better understand the relation between the cell physiological abnormalities and deficits in motor learning, we studied the electrophysiological properties of the output of the cerebellar cortex by recording PC activity in alert animals (Figure 7A). At rest, simple spike (SS) activity in $\alpha6^{Cre}$-*Cacna1a* KO mice was more regular than that of controls as quantified by a significantly decreased coefficient of variance 2 value (CV2; $p = 0.01$; Extended Experimental Procedures), whereas the average SS firing frequency and length of the climbing fiber pause were not significantly different ($p = 0.12$ and $p = 0.59$, respectively) (Figure 7B). In contrast, firing frequency and regularity of complex spike (CS) activity were both normal (all p values >0.5), indicating that spiking activity in the inferior olive is within normal ranges during spontaneous activity (De Zeeuw et al., 2011).

To assess visual processing in the flocculus, which drives plasticity during VOR and OKR adaptation (Ito, 2002; Raymond et al., 1996), we also recorded activity of vertical-axis PCs in alert $\alpha6^{Cre}$-*Cacna1a* KO and WT mice during visual whole-field stimulation at 0.1, 0.4, and 1.6 Hz (Figure 7C). Whereas the timing, i.e., phase, of SS activity relative to the optokinetic stimulus was not significantly different among $\alpha6^{Cre}$-*Cacna1a* KO and WTs

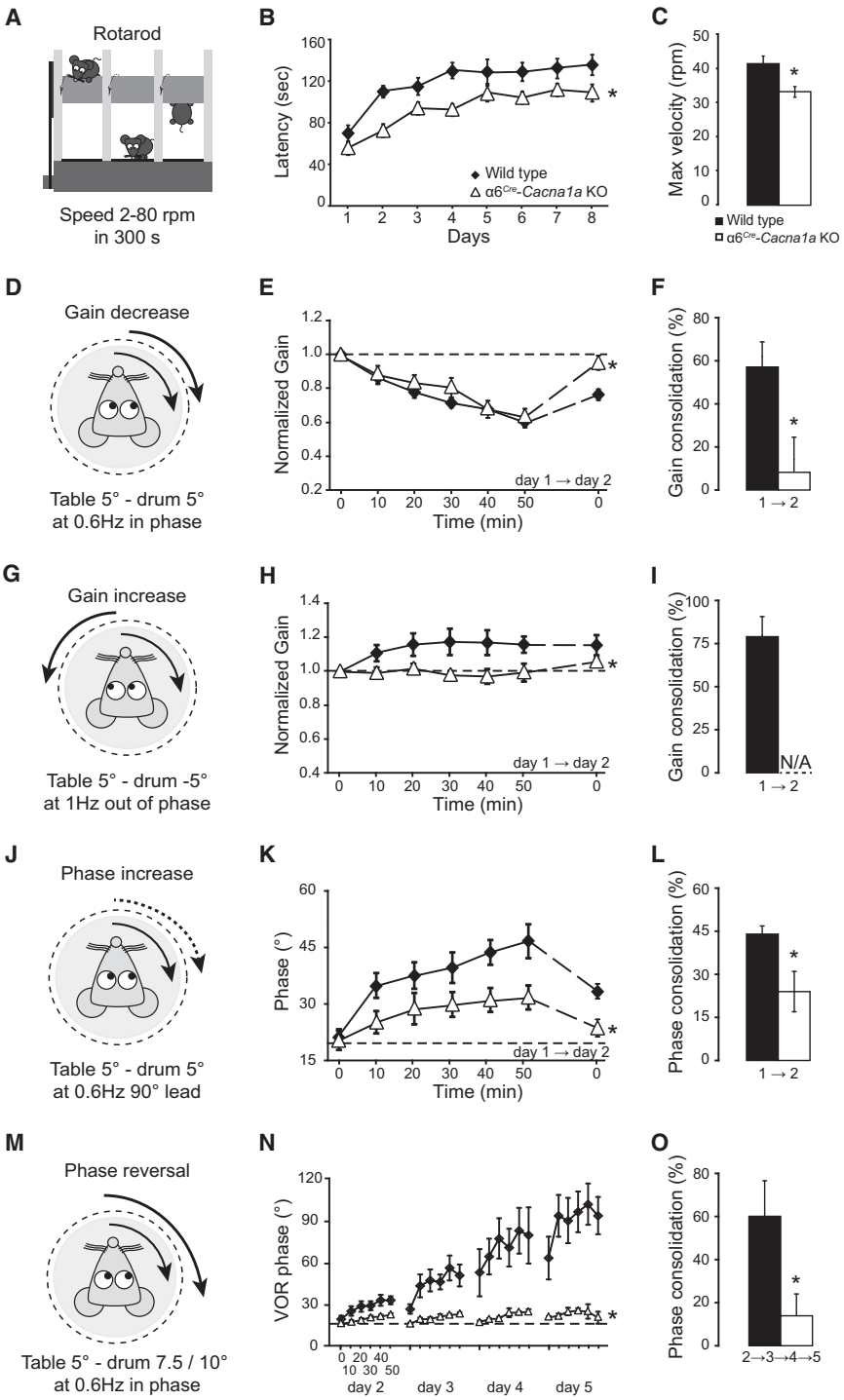

Figure 5. α6^{Cre}-*Cacna1a* KO Mice Show Aberrant Acquisition and Consolidation of Specific Motor Tasks

(A) Representation of rotarod test at 2–80 rpm for 300 s during 8 consecutive days.

(B) Latency to fall (or rotate 360° for three consecutive rotations) for wild-type (black diamond, n = 7) and α6^{Cre}-*Cacna1a* KO mice (white triangle, n = 6).

(C) Maximum rotation speed reached per mouse over the complete training period.

(D) Representation of gain-decrease training paradigm. Day 1: 5 × 10 min sinusoidal, in phase drum and table rotation at 0.6 Hz, both with an amplitude of 5°; day 2: VOR gain measurement at 0.6 Hz.

(E) Normalized gain for VOR recorded with 10 min intervals during 50 min training session for wild-type (black diamond, n = 8) and α6^{Cre}-*Cacna1a* KO mice (white triangle, n = 6) on day 1 and a single measurement at day 2.

(F) Differences in consolidation (percentage change carried forward from the previous day) for gain-decrease training (day 1 to 2).

(G–I) Similar to D-F for gain-increase training for wild-type (n = 8) and α6^{Cre}-*Cacna1a* KO mice (n = 7) (day 1: 5 × 10 min sinusoidal, out-of-phase drum and table rotation at 1.0 Hz, both with an amplitude of 1.6°; day 2: VOR gain measurement at 1.0 Hz).

(J–L) Similar to (D)–(F) for phase-increase training for wild-type (n = 6) and α6^{Cre}-*Cacna1a* KO mice (n = 7) (day 1: 5 × 10 min sinusoidal, drum, and table rotation at 0.6 Hz, and an amplitude of 5°, drum leading table by 90°; day 2: VOR phase measurement at 0.6 Hz).

(M–O), Similar to (D)–(F) for phase-reversal paradigm for wild-type (n = 8) and α6^{Cre}-*Cacna1a* KO mice (n = 6) (following the gain-decrease protocol, from day 2 to day 5: 5 × 10 min sinusoidal in phase drum and table rotation at 0.6 Hz, but with drum amplitudes of 7.5° [days 2 and 3] and 10° [days 4 and 5], while the table amplitude was 5°; gain values are shown in Figure S5A). Phase consolidation over multiple days in O was calculated by dividing the minimal gain or phase change carried onward to day *n* + 1 by the maximal change achieved during day *n*.

The OKR values measured before and after the VOR adaptation are shown in Figures S5B and S5C. Values: mean ± SEM; asterisks: significant differences; p values are described in the main text.

(p = 0.68; repeated-measures ANOVA), both the mean firing rate and modulation amplitude of SS activity of PCs in α6^{Cre}-*Cacna1a* KO were significantly lower during stimulation than those in WT (p < 0.0001 and p = 0.0014, respectively) (Figure 7D). In addition, the magnitude sensitivity of SSs, which corresponds to the spiking activity relative to the eye movement, was significantly lower in α6^{Cre}-*Cacna1a* KO compared to that in WT (p < 0.0001; repeated-measures ANOVA). Moreover, CV and CV2 values of SS activity during modulation were, similar to those during spontaneous activity, significantly reduced (p = 0.0011 and p < 0.00001, respectively; repeated-measures ANOVA). In contrast, the modulation amplitude (p = 0.99; repeated-measures ANOVA), phase (p = 0.51), CV (p = 0.27), and CV2 (p = 0.24) of CS activity during optokinetic stimulation were not significantly different between α6^{Cre}-*Cacna1a* KO and controls, while its mean firing rate during modulation was mildly,

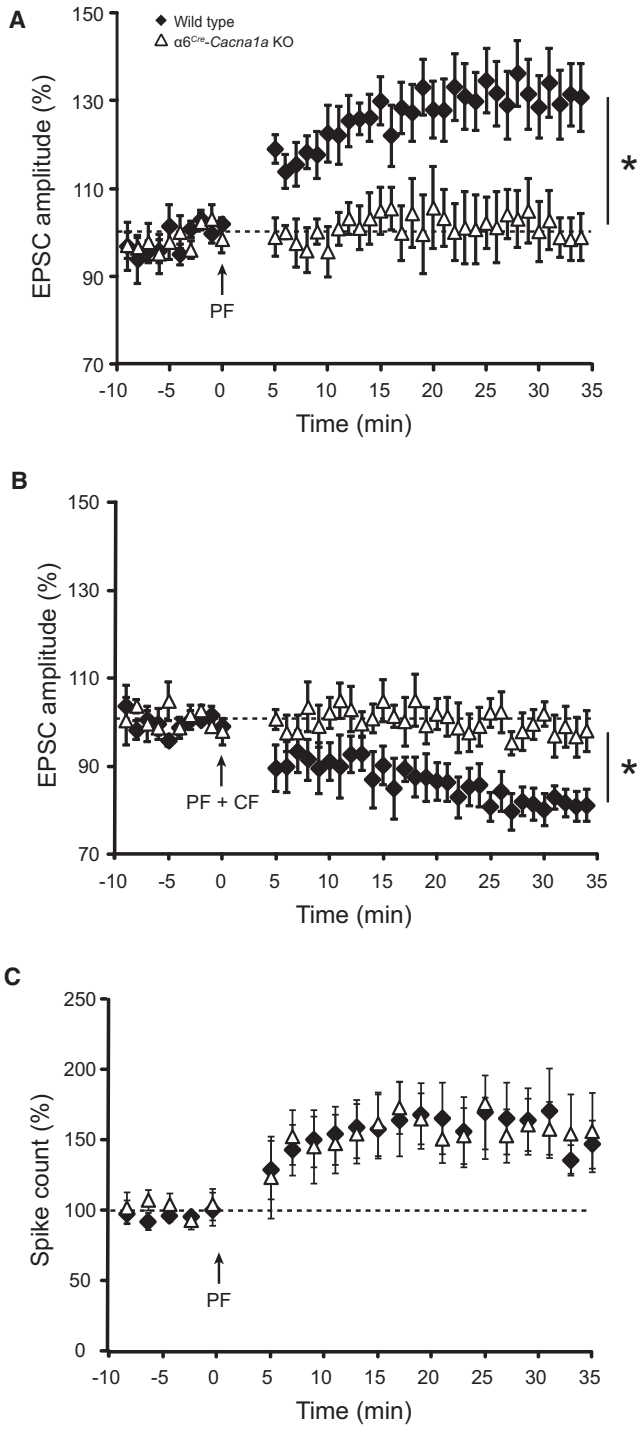

Figure 6. Absent Long-Term Synaptic Plasticity at Parallel Fiber-Purkinje Cell (PF-PC) Synapses, but Normal Intrinsic Plasticity of PC Excitability

(A) Long-term potentiation (LTP) was induced by PF stimulation at 1 Hz for 5 min in wild-type (n = 8) and $\alpha6^{Cre}$-*Cacna1a* KO (n = 6) PCs.

(B) Long-term depression (LTD) was induced by pairing PF and climbing fiber stimulation at 1 Hz for 5 min wild-type (n = 7) and $\alpha6^{Cre}$-*Cacna1a* KO (n = 7).

(C) Plasticity of intrinsic PC excitability was assessed by quantifying the number of action potentials evoked by somatic currents injections before and after PF stimulation at 1 Hz for 5 min in wild-type (n = 8) and $\alpha6^{Cre}$-*Cacna1a* KO (n = 7) PCs.

Values: mean ± SEM; asterisks: significant differences; p values are described in the main text.

but significantly, reduced in $\alpha6^{Cre}$-*Cacna1a* KO PCs (p = 0.04; repeated-measures ANOVA) (Figure 7E). These data indicate that altered SS modulation of PC activity in the flocculus does not necessarily cause a change in motor performance, and they raise the possibility that the deficits in VOR learning and consolidation in $\alpha6^{Cre}$-*Cacna1a* KO mice may result from changes in modulation amplitude and/or regularity of their PC activity.

DISCUSSION

A relatively small subset of functionally intact GCs appears sufficient to maintain basic motor performance, whereas it fails to encode demanding forms of short-term learning and memory consolidation. Toning down the output of the majority of GCs affects induction of both LTP and LTD at the PF to PC synapse, but not the potential of PCs to modify their intrinsic excitability. Likewise, it affects the firing rate, amplitude, and regularity of PC SS activity during modulation, but it does not change the average firing frequency at rest. These findings provide important experimental clues as to why vertebrates need an extreme abundance of functional GCs in daily life and to what extent this abundance is redundant.

Vast Majority of Granule Cells Is Silenced

We successfully generated a cell-specific mouse line that comprises both a minority of intact GCs in which neurotransmission appears normal and a majority of GCs in which neurotransmission is largely impaired due to a lack of functional P/Q-type channels. Despite the fact that this latter defect in GCs did not affect their spontaneous dendritic and somatic activity or that of their postsynaptic target neurons, we found a significant decrease in the overall responses of SCs and PCs to PF beam stimulation. This reduced response level can, in principle, result from a reduced number of functional GCs and/or from a reduced function of GCs. Our blocking experiments with Agatoxin raise the possibility that in the Cre-positive neurons, which lack P/Q-type channels, some fraction of neurotransmitter release might still be functionally intact due to the activation of non-P/Q-type channels. Yet, we have not been able to find direct signs of compensation by N- and R-type channels. In addition, the paired-pulse ratios at both the GC-PC and GC-SC synapses in $\alpha6^{Cre}$-*Cacna1a*KO were not different from those in WT, which probably would not have occurred if the release of neurotransmitters from GCs was mediated by a heterogeneous population of calcium channels (Inchauspe et al., 2004). Moreover, the GC-PC double whole-cell recordings showed that the percentage of connectivity is highly reduced in KO, while there was no significant difference in the amplitude of unitary PC responses to single GC activation. Thus, together with the immunocytochemical and PCR data, which indicated that 75% to 86% of the GCs was affected, our results imply that the reductions in response level of SCs and PCs result mainly from a vastly reduced number of functional GCs.

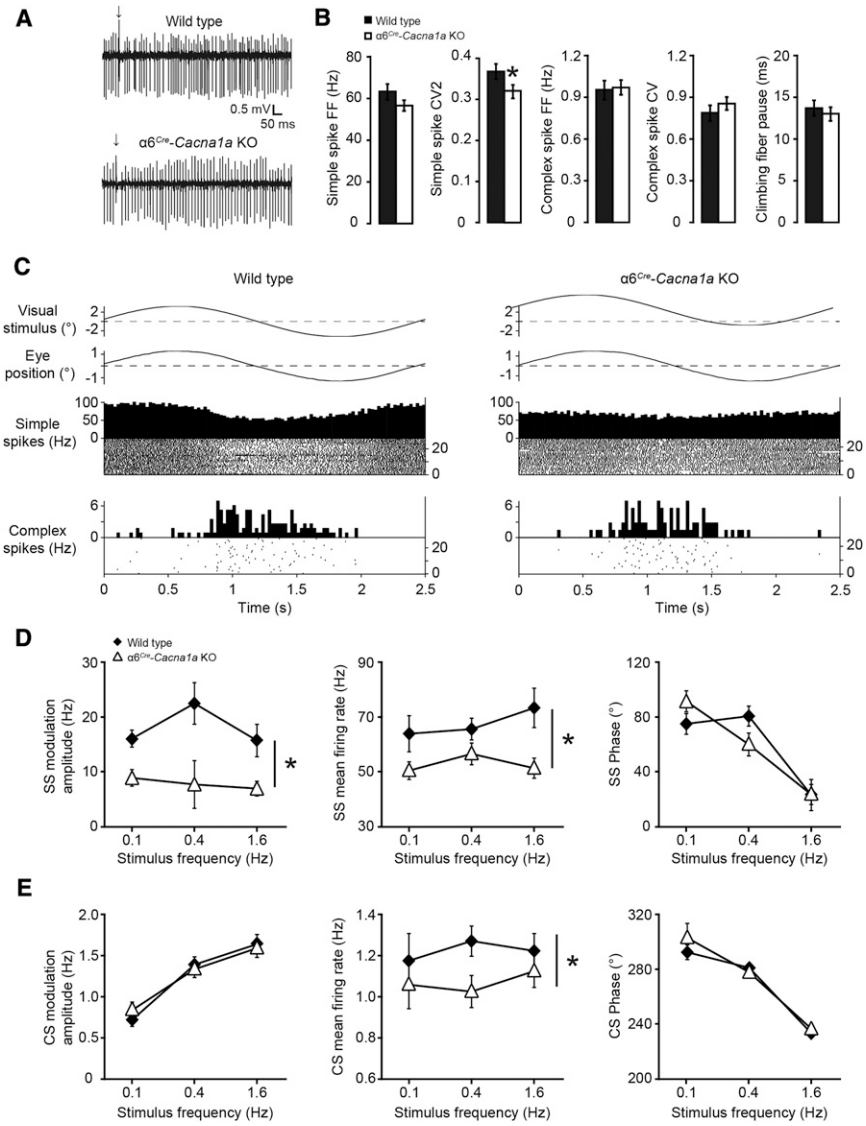

Figure 7. α6^{Cre}-*Cacna1a* KO Mice Show More Regular PC SS Firing and Decreased Modulation of SSs in Response to Optokinetic Stimulation

(A) Example traces of extracellularly recorded PC activity from alert wild-type (left) and α6^{Cre}-*Cacna1a* KO mice (right). Both traces show negative deflections (SSs) and a single positive deflection (CS; arrow) of which the latter is consistently followed by a pause confirming the single-unit character of the recordings.

(B) Average SS firing frequency (FF) and coefficient of variance 2 value (CV2) for wild-type (black, n = 26) and α6^{Cre}-*Cacna1a* KO mice (white, n = 33). Average CS firing frequency and coefficient of variance (CV) and pause in SS firing following CSs, i.e., climbing fiber pause, for the same recordings.

(C) Representative single-unit activity recorded from Purkinje cells in the flocculus of a wild-type (left) and a α6^{Cre}-*Cacna1a* KO (right) mouse during fixed velocity (8°/s, 0.4 Hz) OKR stimulation. The visual stimulus and eye position are shown together with histograms of SS and CS frequencies and corresponding raster plots.

(D) Left: amplitude of SS modulation recorded in response to optokinetic stimulation at 0.1 Hz (WT: n = 11; KO: n = 9), 0.4 Hz (WT: n = 13; KO: n = 13), and 1.6 Hz (WT: n = 8; KO: n = 9). Middle: mean SS firing rate during modulation. Right: phase of SS modulation relative to the stimulus.

(E) CS amplitude, mean firing rate, and phase of modulation.

Significance was tested using a nonorthogonal repeated-measure ANOVA (Extended Experimental Procedures).

Values: mean ± SEM; asterisks: significant differences; p values are described in the main text.

Abundance of Granule Cells Is Required for Dynamic Range and Temporal Variation of PC Activity as Well as Motor Learning and Consolidation

Our data show that one can substantially reduce the GC output and yet merely induce deficits in particular forms of learning and consolidation without causing deficits in motor performance. This finding is particularly surprising if one takes into account that the SS rate coding of floccular PCs in α6^{Cre}-*Cacna1a* KOs was affected during normal optokinetic eye movements. Probably, the decreases in mean firing rate and amplitude of the SS activity result from both a reduction of GC output directly onto Purkinje cells and a reduced inhibitory input onto PCs from MLIs, which also received a reduced GC input. The reduction in SS activity during modulation presumably disinhibits neurons in the cerebellar and vestibular nuclei and thereby increases the inhibitory input to olivary neurons (Best and Regehr, 2009; Chen et al., 2010), which might explain the slight reduction of CS firing rate during modulation. Apparently, the reduced SS activity and CS activity in α6^{Cre}-*Cacna1a* KO mice during natural (i.e., nonmismatch, nontraining) visual and vestibular stimulation were sufficient to control the modulation in downstream targets at such a level that the amplitude and timing of the movements during baseline OKR and VOR were functionally adequate. Possibly, compensatory mechanisms at the cerebellar nuclei facilitated by collateral input from mossy fibers and/or climbing fibers play a conserving role during normal motor performance (De Zeeuw et al., 2011). Yet, during more challenging paradigms, such as locomotion learning on a fast-accelerating rotarod or gain-increase and phase-reversal learning of the VOR, the cerebellar system appears to need a wider dynamic range of SS modulations of its PCs to entrain its target neurons downstream (Aizenman and Linden, 2000; Medina and Lisberger, 2008; Nelson et al., 2003). Similarly, the difference in temporal variability (i.e., CV2 value) of SS activity in α6^{Cre}-*Cacna1a* KO mice was apparently not detrimental for motor performance, whereas it might have contributed to some of the learning and consolidation deficits (Seja et al., 2012; Wulff et al., 2009). It is interesting to note that modifications

of calcium kinetics in GCs with presumably opposite effects on calcium influx can actually increase SS activity and concomitantly affect motor performance (Bearzatto et al., 2006; Schiffmann et al., 1999). These modifications of calretinin expression did not directly affect neurotransmission at the parallel fiber synapses, but instead increased the excitability of GCs, while altering the climbing fiber pause together with SS activity (Bearzatto et al., 2006; Gall et al., 2003; Schiffmann et al., 1999).

Our finding that abundant numbers of GCs are required to sustain a sufficient dynamic range of SS modulation and temporal variation, which can be called into play during cerebellar motor learning and consolidation, is in line with various models. For example, the Schweighofer model on unsupervised learning of GC sparse coding predicts that basic motor performance can be normal despite a lower number of GCs, whereas the level of learning and stability of learned responses, i.e., consolidation, should be affected as a consequence of a reduced capacity for effective plasticity inside the granular layer (Andreescu et al., 2011; Schweighofer et al., 2001; Seja et al., 2012). Likewise, the Marr-Albus-Ito model predicts that plasticity at the PF-PC synapse is critical for motor learning (Ito, 2002), while Lisberger's model on VOR learning is consistent with a dynamic role for rate coding in SS responses (Ramachandran and Lisberger, 2008). Finally, a recent model from our own group predicts that proper spatiotemporal patterns of SS activity may contribute to consolidation of motor learning in the nuclei downstream (De Zeeuw et al., 2011; Wulff et al., 2009).

Emerging Hypothesis of Distributed Synergistic Plasticity

A closer look at the precise cell physiological and behavioral phenotypes in the current GC-specific $\alpha6^{Cre}$-*Cacna1a* KO mouse and a direct comparison with those of other cerebellar mouse mutants point toward a common hypothesis on distributed synergistic plasticity as the main mechanism underlying cerebellar learning (Gao et al., 2012). For example, when we blocked the induction of PF LTD by inhibiting PKC activity in PCs we found, unlike in the $\alpha6^{Cre}$-*Cacna1a* KO, a phenotype in VOR gain-decrease learning (De Zeeuw et al., 1998; van Alphen and De Zeeuw, 2002). This discrepancy may be explained by the fact that PKC operates at many sites inside PCs including its dendrites, cell body, and axon terminals, and thus blockage of PKC in PCs may have, apart from minimizing PF LTD, various effects such as impairing plasticity at the MLI to PC synapse and/or at the PC to cerebellar nucleus neuron synapse (Kano et al., 1996; Pedroarena and Schwarz, 2003; Song and Messing, 2005). A similar argument of synergistic interactions with other forms of plasticity may also explain why we did not find any behavioral phenotype when we blocked the expression of LTD by impairing internalization of AMPA receptors (Schonewille et al., 2011); here, plasticity at the MLI to PC synapse was probably unaffected and thus formed a potential site for compensation. Or similarly, in L7-PP2B mice, in which both postsynaptic PF-PC LTP and PC intrinsic plasticity are affected, we found deficits not only in gain increase, but also, differently from the $\alpha6^{Cre}$-*Cacna1a* KOs, in gain-decrease learning (Schonewille et al., 2010). Therefore, we hypothesize that plasticity at PF-PC synapses may contribute to learning under normal physiological circumstances, but that it is not essential for it and that its blockage can be compensated for by plasticity at other synaptic sites and/or by plasticity of intrinsic excitability of PCs or downstream neurons. This hypothesis of distributed synergistic plasticity could also explain why we have both a learning and consolidation phenotype in $\alpha6^{Cre}$-*Cacna1a* KOs. In this mouse mutant, the direct route from GCs to PCs as well as the indirect route via the interneurons to PCs is affected. In this respect, it is interesting to note that L7-γ2 KO mice, which suffer from a block of inhibition onto PCs and, as a secondary effect, a reduced PF excitatory input (Wulff et al., 2009), have a deficit in eye-movement performance, whereas $\alpha6^{Cre}$-*Cacna1a* KOs do not have such a deficit, but show instead a phenotype in gain-increase learning.

Finally, the concept of distributed synergistic plasticity may also help to explain why it is possible that a mouse mutant like the $\alpha6^{Cre}$-*Cacna1a* KO does not show any deficit in regular motor performance, while it does have impairments in motor learning. One of the main reasons is probably that different forms of plasticity require different periods of time to be fully induced and expressed (Gao et al., 2012). As a consequence, behavioral deficits can start to arise in the lab when animals are challenged to learn a new task in a relatively short time, such as learning a new gain and/or phase of its eye movements within a couple of hours, during which only some forms of plasticity can be engaged. Instead, in real life the mutant has weeks to compensate and use all other forms of plasticity including those that may operate slower than the specific type of plasticity affected and those that do not even reside within the cerebellar cortex. This implies that the mutant will learn at a slower pace, but eventually it can lead to a normal baseline motor performance. The differences in learning deficits during short-term and long-term training periods found for L7-PKCi mutants are in line with this hypothesis (De Zeeuw et al., 1998; van Alphen and De Zeeuw, 2002). Thus, together with the phenotypes of other cell-specific mutants of the cerebellar cortex, the current data obtained with the $\alpha6^{Cre}$-*Cacna1a* KO point toward the possibility that the plasticity mechanisms underlying cerebellar learning are distributed in that they occur at multiple sites and operate over time in a synergistic fashion in that they can reinforce one another and allow for compensation.

Implications of Sparse Coding Inside and Outside the Cerebellum for Memory Formation

Apart from the numerical changes in connectivity of their granular and molecular layer, configuration changes in the network that affect sparse coding may also contribute to the aberrant acquisition and consolidation of long-term memory in $\alpha6^{Cre}$-*Cacna1a* KO mice. An important factor might be that silencing GCs in a random fashion scatters the GC output to PCs into a mosaic pattern. This scattering of GC output might not only directly corrupt the potential of PCs to integrate spatiotemporal encodings, but it may also contribute to the disrupted synaptic plasticity between GCs and PCs, which may require a specific clustering of inputs to be induced successfully (Eilers et al., 1995). In principle, the putatively detrimental effects of a lack of spatial clustering may apply to both LTD and LTP induction at the PF-PC synapses, both of which were affected in

$\alpha6^{Cre}$-*Cacna1a* KO mice. The reduction in spatial clustering of GC output may thus push the cerebellar system to such an extreme sparseness that it corrupts the formation of appropriate activity patterns rather than being functional for memory storage (Wilms and Hausser, 2010, FENS, abstract).

In the present study, the usefulness of cell-specific subtotal genetic lesions is revealed by the fact that one of the main functions of the cerebellum, i.e., control of motor performance, is not affected by the lesion, whereas its other two main functions, i.e., motor learning and consolidation, are affected. These data stand in contrast to those obtained with lesions of all GCs, which result in severe ataxia and learning deficits (De Zeeuw et al., 2004; Kim et al., 2009). The subtotal, but cell-specific, approach has also provided interesting results in other memory systems. For example, subtotal genetic lesions of the entorhinal cortex layer III cells that provide input to the hippocampus impairs the temporal association memory tasks, but not the acquisition, recall, or consolidation of spatial reference memory (Suh et al., 2011). Or at an even more precise quantitative level, fear-conditioning memory can be affected by a blockage of AMPA receptor synaptic incorporation in as few as ~15% of the neuronal population in the lateral amygdala or by deleting a similarly small subpopulation of CREB-expressing neurons in the same region (Han et al., 2009; Rumpel et al., 2005). Thus, in line with these studies on declarative memories formed by extracerebellar regions, the current study on the granular layer of the cerebellum shows that sparseness of coding is more relevant for formation and consolidation of procedural memories than for other basic cerebellar functions such as control of motor performance, for which the network has a higher level of redundancy.

EXPERIMENTAL PROCEDURES

Generation of $\alpha6^{Cre}$-*Cacna1a* KO Mice

Mutant mice lacking P/Q-type VGCCs in GCs were obtained crossing mice carrying a floxed Cacna1a allele (exon 4) (Todorov et al., 2006) with mice carrying the $\alpha6$-*Cre* transgene (Aller et al., 2003). Mice of the following genotypes were used for the experiments: *Cacna1a*$^{LoxP/LoxP}$/*Cre*+ (i.e., $\alpha6^{Cre}$-*Cacna1a* KO) and *Cacna1a*$^{LoxP/LoxP}$/*Cre*−, *Cacna1a*$^{wt/wt}$/*Cre*+ and *Cacna1a*$^{wt/wt}$/*Cre*− (i.e., wild-type). For all experiments, the researchers were blind to the genotype of the animals (all older than P18, gender-matched for behavioral experiments). All experiments were performed in accordance with the guidelines for animal experiments of the respective universities and the Dutch national legislation.

Quantitative PCR

The efficiency of *Cacna1a* deletion was determined by performing quantitative PCR on DNA isolated from cerebella, cortices, and lungs of *Cacna1a*$^{LoxP/LoxP}$/Cre+ and *Cacna1a*$^{LoxP/LoxP}$/Cre mice. QPCR primer sets were chosen for the identification of the first LoxP site (nonrecombined allele) and a reverse primer set downstream of the second LoxP site (recombined allele).

Immunohistochemistry and Electron Microscopy

The primary antibody mouse anti-Cre (MMS-106P, Covance) was detected with a biotinylated goat anti-mouse secondary antibody (Sigma-Aldrich, Netherlands). The staining was visualized with the avidin-biotin-peroxidase complex method (Vector Laboratories) and 0.05% diaminobenzidine as the chromogen. Neuronal morphology was assessed using a rapid GolgiStain Kit (FD Neurotechnologies) and Neurolucida software (Microbrightfield). For electron microscopy sections were processed as described before (De Zeeuw et al., 1998). Micrographs were taken at 2,600× (granular layer) or at 25,000× (distalmolecular layer). Quantitative analysis was performed with MetaVue 4.6 (Metavue Corporation).

In Vitro Electrophysiology

Sagittal slices of cerebellar vermis (250 μm) were made in ice-cold oxygenated "slicing" solution and kept at room temperature (RT, 21°C ± 2°C) in oxygenated artificial cerebrospinal fluid (ACSF). Whole-cell patch-clamp recordings were performed at RT using an Axopatch 700B (Molecular Devices, USA) or an EPC-10 amplifier (HEKA, Germany) in the presence of 100 μM picrotoxin. Using patch electrodes filled with ACSF, we stimulated PFs in the outer one-third of the molecular layer, CFs in the granular layer and MFs in the white matter. Recordings were excluded if series or input resistances (assessed by −10 mV voltage steps following each test pulse) varied by >15%.

Motor Behavior

After a week of handling, the motor behavior was tested with four paradigms: (1) locomotion in an open field, (2) motor coordination on an accelerating rotating rod (40/80 rpm) for maximal eight consecutive days, (3) balancing on a 1.5 cm wide beam, and (4) walking pattern for 4 consecutive days on the Erasmus ladder.

Compensatory Eye Movements

After 5 days of recovery following placement of a skull pedestal, mice were fixed onto the center of a turntable surrounded by a cylindrical screen. Baseline OKR and (V)VOR were evoked by rotating either the screen with a constant velocity of 8°/s or the turntable with a constant amplitude of 5°. Adaptation protocols are listed in the figure legends.

In Vivo Electrophysiology

PCs were identified by their brief pause in SS activity following each CS and recorded extracellularly from either the flocculus or nonfloccular regions in a lighted surrounding. The optimal axis tomodulate floccular Purkinje cell activity was determined by rotating the planetarium around the vertical axis or a horizontal axis at 135° azimuth, ipsilateral to the side of recording (Schonewille et al., 2010).

Data analysis

All values are represented as mean ± SEM; p values of <0.05 were considered significant and are reported in the main text. Statistical analysis was done using Student's t test, unless stated otherwise.

SUPPLEMENTAL INFORMATION

Supplemental Information includes Extended Experimental Procedures, five figures, and four tables and can be found with this article online at http://dx.doi.org/10.1016/j.celrep.2013.03.023.

LICENSING INFORMATION

ACKNOWLEDGMENTS

We are grateful to E. Haasdijk, M. Rutteman, P. Plak, R. Avila Freire, Dr. E. Mientjes (Erasmus MC), and L. Broos (LUMC) for technical assistance and to Dr. B.J. van Beugen, Prof. G. Borst, Prof. Y. Elgersma (Erasmus MC), Prof. R.A. Silver (UCL), and Prof. W. Regher (Harvard) for critical discussions. This work was supported by the Dutch Organization for Medical Sciences (ZonMw; F.E.H., A.M.J.M.v.d.M., and C.I.D.Z.), Life Sciences (ALW; F.E.H., C.I.D.Z.), Erasmus University Fellowship (M.S., F.E.H.), Senter (Neuro-Basic), ERC-adv, CEREBNET, and C7 programs of the EU (C.I.D.Z.), and EU "EUROHEAD" and Centre for Medical Systems Biology (A.M.J.M.v.d.M.).

Cell PRESS
Open ACCESS

Received: August 26, 2012
Revised: January 30, 2013
Accepted: March 15, 2013
Published: April 11, 2013

REFERENCES

Aizenman, C.D., and Linden, D.J. (2000). Rapid, synaptically driven increases in the intrinsic excitability of cerebellar deep nuclear neurons. Nat. Neurosci. *3*, 109–111.

Aller, M.I., Jones, A., Merlo, D., Paterlini, M., Meyer, A.H., Amtmann, U., Brickley, S., Jolin, H.E., McKenzie, A.N., Monyer, H., et al. (2003). Cerebellar granule cell Cre recombinase expression. Genesis *36*, 97–103.

Andreescu, C.E., Prestori, F., Brandalise, F., D'Errico, A., De Jeu, M.T., Rossi, P., Botta, L., Kohr, G., Perin, P., D'Angelo, E., and De Zeeuw, C.I. (2011). NR2A subunit of the N-methyl D-aspartate receptors are required for potentiation at the mossy fiber to granule cell synapse and vestibulo-cerebellar motor learning. Neuroscience *176*, 274–283.

Bearzatto, B., Servais, L., Roussel, C., Gall, D., Baba-Aissa, F., Schurmans, S., de Kerchove d'Exaerde, A., Cheron, G., and Schiffmann, S.N. (2006). Targeted calretinin expression in granule cells of calretinin-null mice restores normal cerebellar functions. FASEB J. *20*, 380–382.

Belmeguenai, A., Hosy, E., Bengtsson, F., Pedroarena, C.M., Piochon, C., Teuling, E., He, Q., Ohtsuki, G., De Jeu, M.T., Elgersma, Y., et al. (2010). Intrinsic plasticity complements long-term potentiation in parallel fiber input gain control in cerebellar Purkinje cells. J. Neurosci. *30*, 13630–13643.

Best, A.R., and Regehr, W.G. (2009). Inhibitory regulation of electrically coupled neurons in the inferior olive is mediated by asynchronous release of GABA. Neuron *62*, 555–565.

Chadderton, P., Margrie, T.W., and Häusser, M. (2004). Integration of quanta in cerebellar granule cells during sensory processing. Nature *428*, 856–860.

Chen, C., and Regehr, W.G. (1997). The mechanism of cAMP-mediated enhancement at a cerebellar synapse. J. Neurosci. *17*, 8687–8694.

Chen, X., Kovalchuk, Y., Adelsberger, H., Henning, H.A., Sausbier, M., Wietzorrek, G., Ruth, P., Yarom, Y., and Konnerth, A. (2010). Disruption of the olivo-cerebellar circuit by Purkinje neuron-specific ablation of BK channels. Proc. Natl. Acad. Sci. USA *107*, 12323–12328.

D'Angelo, E., De Filippi, G., Rossi, P., and Taglietti, V. (1997). Synaptic activation of Ca2+ action potentials in immature rat cerebellar granule cells in situ. J. Neurophysiol. *78*, 1631–1642.

De Zeeuw, C.I., Hansel, C., Bian, F., Koekkoek, S.K., van Alphen, A.M., Linden, D.J., and Oberdick, J. (1998). Expression of a protein kinase C inhibitor in Purkinje cells blocks cerebellar LTD and adaptation of the vestibulo-ocular reflex. Neuron *20*, 495–508.

De Zeeuw, C.I., Koekoek, S.K.E., Van Alphen, A.M., Luo, C., Hoebeek, F.E., Van der Steen, J., Frens, M.A., Sun, J., Goossens, H.H.L.M., Jaarsma, D., et al. (2004). Gain and phase control of compensatory eye movements by the vestibulo-cerebellar system. In Handbook of Auditory Research, S.M. Highstein, R.R. Fay, and A.N. Popper, eds. (New York: Springer-Verlag).

De Zeeuw, C.I., Hoebeek, F.E., Bosman, L.W., Schonewille, M., Witter, L., and Koekkoek, S.K. (2011). Spatiotemporal firing patterns in the cerebellum. Nat. Rev. Neurosci. *12*, 327–344.

Eccles, J.C. (1969). The development of the cerebellum of vertebrates in relation to the control of movement. Naturwissenschaften *56*, 525–534.

Eilers, J., Augustine, G.J., and Konnerth, A. (1995). Subthreshold synaptic Ca2+ signalling in fine dendrites and spines of cerebellar Purkinje neurons. Nature *373*, 155–158.

Ekerot, C.F., and Jörntell, H. (2008). Synaptic integration in cerebellar granule cells. Cerebellum *7*, 539–541.

Gall, D., Roussel, C., Susa, I., D'Angelo, E., Rossi, P., Bearzatto, B., Galas, M.C., Blum, D., Schurmans, S., and Schiffmann, S.N. (2003). Altered neuronal excitability in cerebellar granule cells of mice lacking calretinin. J. Neurosci. *23*, 9320–9327.

Gao, Z., van Beugen, B.J., and De Zeeuw, C.I. (2012). Distributed synergistic plasticity and cerebellar learning. Nat. Rev. Neurosci. *13*, 619–635.

Han, J.H., Kushner, S.A., Yiu, A.P., Hsiang, H.L., Buch, T., Waisman, A., Bontempi, B., Neve, R.L., Frankland, P.W., and Josselyn, S.A. (2009). Selective erasure of a fear memory. Science *323*, 1492–1496.

Hansel, C., de Jeu, M., Belmeguenai, A., Houtman, S.H., Buitendijk, G.H., Andreev, D., De Zeeuw, C.I., and Elgersma, Y. (2006). alphaCaMKII Is essential for cerebellar LTD and motor learning. Neuron *51*, 835–843.

Inchauspe, C.G., Martini, F.J., Forsythe, I.D., and Uchitel, O.D. (2004). Functional compensation of P/Q by N-type channels blocks short-term plasticity at the calyx of held presynaptic terminal. J. Neurosci. *24*, 10379–10383.

Ito, M. (2002). Historical review of the significance of the cerebellum and the role of Purkinje cells in motor learning. Ann. N Y Acad. Sci. *978*, 273–288.

Kano, M., Kano, M., Fukunaga, K., and Konnerth, A. (1996). Ca(2+)-induced rebound potentiation of gamma-aminobutyric acid-mediated currents requires activation of Ca2+/calmodulin-dependent kinase II. Proc. Natl. Acad. Sci. USA *93*, 13351–13356.

Kim, J.C., Cook, M.N., Carey, M.R., Shen, C., Regehr, W.G., and Dymecki, S.M. (2009). Linking genetically defined neurons to behavior through a broadly applicable silencing allele. Neuron *63*, 305–315.

Maricich, S.M., Soha, J., Trenkner, E., and Herrup, K. (1997). Failed cell migration and death of purkinje cells and deep nuclear neurons in the weaver cerebellum. J. Neurosci. *17*, 3675–3683.

Medina, J.F., and Lisberger, S.G. (2008). Links from complex spikes to local plasticity and motor learning in the cerebellum of awake-behaving monkeys. Nat. Neurosci. *11*, 1185–1192.

Mintz, I.M., Sabatini, B.L., and Regehr, W.G. (1995). Calcium control of transmitter release at a cerebellar synapse. Neuron *15*, 675–688.

Myoga, M.H., and Regehr, W.G. (2011). Calcium microdomains near R-type calcium channels control the induction of presynaptic long-term potentiation at parallel fiber to purkinje cell synapses. J. Neurosci. *31*, 5235–5243.

Nelson, A.B., Krispel, C.M., Sekirnjak, C., and du Lac, S. (2003). Long-lasting increases in intrinsic excitability triggered by inhibition. Neuron *40*, 609–620.

Pedroarena, C.M., and Schwarz, C. (2003). Efficacy and short-term plasticity at GABAergic synapses between Purkinje and cerebellar nuclei neurons. J. Neurophysiol. *89*, 704–715.

Ramachandran, R., and Lisberger, S.G. (2008). Neural substrate of modified and unmodified pathways for learning in monkey vestibuloocular reflex. J. Neurophysiol. *100*, 1868–1878.

Raymond, J.L., Lisberger, S.G., and Mauk, M.D. (1996). The cerebellum: a neuronal learning machine? Science *272*, 1126–1131.

Rothman, J.S., Cathala, L., Steuber, V., and Silver, R.A. (2009). Synaptic depression enables neuronal gain control. Nature *457*, 1015–1018.

Rumpel, S., LeDoux, J., Zador, A., and Malinow, R. (2005). Postsynaptic receptor trafficking underlying a form of associative learning. Science *308*, 83–88.

Schiffmann, S.N., Cheron, G., Lohof, A., d'Alcantara, P., Meyer, M., Parmentier, M., and Schurmans, S. (1999). Impaired motor coordination and Purkinje cell excitability in mice lacking calretinin. Proc. Natl. Acad. Sci. USA *96*, 5257–5262.

Schonewille, M., Belmeguenai, A., Koekkoek, S.K., Houtman, S.H., Boele, H.J., van Beugen, B.J., Gao, Z., Badura, A., Ohtsuki, G., Amerika, W.E., et al. (2010). Purkinje cell-specific knockout of the protein phosphatase PP2B impairs potentiation and cerebellar motor learning. Neuron *67*, 618–628.

Schonewille, M., Gao, Z., Boele, H.J., Veloz, M.F., Amerika, W.E., Simek, A.A., De Jeu, M.T., Steinberg, J.P., Takamiya, K., Hoebeek, F.E., et al. (2011). Reevaluating the role of LTD in cerebellar motor learning. Neuron *70*, 43–50.

Schweighofer, N., Doya, K., and Lay, F. (2001). Unsupervised learning of granule cell sparse codes enhances cerebellar adaptive control. Neuroscience *103*, 35–50.

Seja, P., Schonewille, M., Spitzmaul, G., Badura, A., Klein, I., Rudhard, Y., Wisden, W., Hübner, C.A., De Zeeuw, C.I., and Jentsch, T.J. (2012). Raising

cytosolic Cl- in cerebellar granule cells affects their excitability and vestibulo-ocular learning. EMBO J. *31*, 1217–1230.

Sidman, R.L., Green, M.C., and Appel, S.H. (1965). Catalog of the neurological mutants of the mouse (Cambridge, Mass.: Harvard University Press).

Song, M., and Messing, R.O. (2005). Protein kinase C regulation of GABAA receptors. Cell. Mol. Life Sci. *62*, 119–127.

Suh, J., Rivest, A.J., Nakashiba, T., Tominaga, T., and Tonegawa, S. (2011). Entorhinal cortex layer III input to the hippocampus is crucial for temporal association memory. Science *334*, 1415–1420.

Todorov, B., van de Ven, R.C., Kaja, S., Broos, L.A., Verbeek, S.J., Plomp, J.J., Ferrari, M.D., Frants, R.R., and van den Maagdenberg, A.M. (2006). Conditional inactivation of the Cacna1a gene in transgenic mice. Genesis *44*, 589–594.

Tymms, M.J., and Kola, I. (2001). Gene knockout protocols (New York: Humana Press).

van Alphen, A.M., and De Zeeuw, C.I. (2002). Cerebellar LTD facilitates but is not essential for long-term adaptation of the vestibulo-ocular reflex. Eur. J. Neurosci. *16*, 486–490.

Wada, N., Kishimoto, Y., Watanabe, D., Kano, M., Hirano, T., Funabiki, K., and Nakanishi, S. (2007). Conditioned eyeblink learning is formed and stored without cerebellar granule cell transmission. Proc. Natl. Acad. Sci. USA *104*, 16690–16695.

Williams, R.W., and Herrup, K. (1988). The control of neuron number. Annu. Rev. Neurosci. *11*, 423–453.

Wulff, P., Schonewille, M., Renzi, M., Viltono, L., Sassoè-Pognetto, M., Badura, A., Gao, Z., Hoebeek, F.E., van Dorp, S., Wisden, W., et al. (2009). Synaptic inhibition of Purkinje cells mediates consolidation of vestibulo-cerebellar motor learning. Nat. Neurosci. *12*, 1042–1049.